7860 *Macromolecules* **2010**, *43*, 7860–7863
DOI: 10.1021/ma101570u

Macromolecules
NOTE

β Phase Formation in Poly(9,9-di-*n*-decylfluorene) Thin Films

Daniel W. Bright,[†] Frank Galbrecht,[‡] Ullrich Scherf,[‡] and Andrew P. Monkman*,[†]

[†]*Department of Physics, Durham University, South Road, Durham DH1 3LE, U.K., and* [‡]*Institut für Polymertechnologie, Makromolekulare Chemie, Bergische Universität Wuppertal, Gauss-Str. 20, 42097 Wuppertal, Germany*

Received July 14, 2010; Revised Manuscript Received August 6, 2010

The polymer poly(9,9-di-*n*-octylfluorene) (PFO or PF8) has been well studied for its excellent emission properties including polarized emission[1−3] and high fluorescence efficiency.[4] The polymer is noted for the formation of a highly ordered phase, termed the β phase, upon thermal cycling from low temperature and back up to room temperature[2,5,6] or exposure to toluene vapor.[2] This phase is composed of polymer backbones with a more planar configuration, where the helical twist of the repeat units along the chain has unwound,[7,8] which extends the mean conjugation length and thus leads to a red-shifted absorption and emission bands.[9] This low-energy phase readily traps excitons via strong Förster transfer and exciton migration.[10,11] This gives rise to sharp and well-resolved emission spectra and even strong amplified spontaneous emission from the β phase via pumping of the α phase.[12]

For a long time, it was thought that only the dioctyl-substituted polyfluorene, i.e. PF8, was able to form the β phase.[13] However, we recently demonstrated the formation of the β phase in a group of polymers identical to PF8 but having different linear alkyl side chain lengths ranging from 6 to 10 carbon atoms, named PF6 to PF10.[15] In solution, X-ray studies revealed the formation of sheets of "aggregate" in MCH solution (a moderate solvent for polyfluorenes) for PF6 to PF9, but not PF10.[14] Corresponding work on temperature-dependent optical spectra showed the β phase forms in the cases of PF7, PF8, and PF9 solutions in MCH only,[15] leading to the proposal that while aggregation occurs alongside the formation of the β phase, the planarization of the backbone is driven by side chain interactions in the solution and the two are separate processes.[16] For side chain lengths of 9 or more carbon atoms, the solvent begins to break up or prevent the aggregate from forming in solution, indicative of a competition between side chain van der Waals forces and the solvent or thermal disruption of these bonds. The work reported in this Note carries on from the earlier studies we have reported in refs 14 and 15 and adds new data on β phase formation in PF10 as well.

In films of these polymers, there is no solvent present to prevent interactions between the longer side chain polymer, and so it might be possible that β phase may form to some extent in the polymer poly(9,9-di-*n*-decylfluorene) or PF10. Data presented in this Note show that indeed the β phase does form in thin films of PF10 to some extent, but the extent of planarization is limited, most likely by the hindrance of neighboring chains limiting the amount of local-scale movement that is needed to allow the interdigitation of the side chains.

However, it should be remembered that the length of the alkyl chains is the main controlling factor to β phase formation. The alkyl chains lie perpendicular to the backbone of the phenyl rings, and so the phenyl rings will also be perpendicular to the plane of the β phase lamella; thus, any phenyl−phenyl ring interaction will be from the rings "inside" the side chain lamella and will be weak through the incumbent staggering of adjacent chain phenyl rings. This then also explains why the β phase lamella are effectively pure two-dimensional entities as the only interplane interactions would be very weak.[7,8] However, this new observation adds further evidence to the conclusion drawn in our earlier work[15] that the β phase formation is controlled by side chain interactions.

Experimental Section

PF10 was synthesized following the procedure outlined in ref 10. Thin films were made by spinning from solutions of PF10 at 10 mg/mL in toluene at 2000 rpm for 60 s onto 1 mm thick sapphire substrates. Two separate batches of PF10 were used, with M_w ~150 kDa.

Thermal cycling was carried out in a liquid helium closed-loop cryostat with cooling and heating rates of ~0.7 K/min. The heater was controlled by a Scientific Instruments model 9700 temperature controller. The sapphire substrates were carefully mounted into the recessed copper coldfinger using indium wire to thermally anchor the substrate to the coldfinger.

The emission (excited at 380 and 428 nm) and excitation (monitored at 470 nm) spectra were collected in a double-monochromated Jobin-Yvon Fluorolog-3 spectrometer using 0.5 nm intervals at 11 K and 1 nm intervals at other temperatures. Measuring both emission and excitation in the fluorimeter enables changes in both the absorption and emission spectrum to be monitored simultaneously at any temperature.

The films were exposed to high-density toluene vapor by mounting the sample face down in a clamp stand 5 cm above the surface of a toluene bath on a hot plate set to 120 °C. The toluene, used as supplied from Romil, evaporates quickly without boiling at this temperature. The sample clamp was suspended down into the enclosed volume of a 600 mL beaker in order to ensure a stream of vapor passing the film surface and to reduce variations from air drafts. The exposure time was kept to 15 min, and the samples were dried in a stream of compressed air upon removal from the vapor.

The photoluminescence lifetime was measured using a Stanford optics streak camera with pulsed excitation at 390 nm from a mode-locked Ti:sapphire laser. The lifetimes were measured at the emission peak using a biexponential fit to the intensity decay over a 4 ns time window.

Results

Thermal Cycling of Thin Films. The excitation spectra of PF10 films during the cooling cycle are shown in Figure 1. Two identical data sets show the growing in of an excitation shoulder at 429 nm, below the $\pi-\pi^*$ edge, after slowly warming the films back to room temperature. This resembles

---

*Corresponding author. E-mail: a.p.monkman@durham.ac.uk.

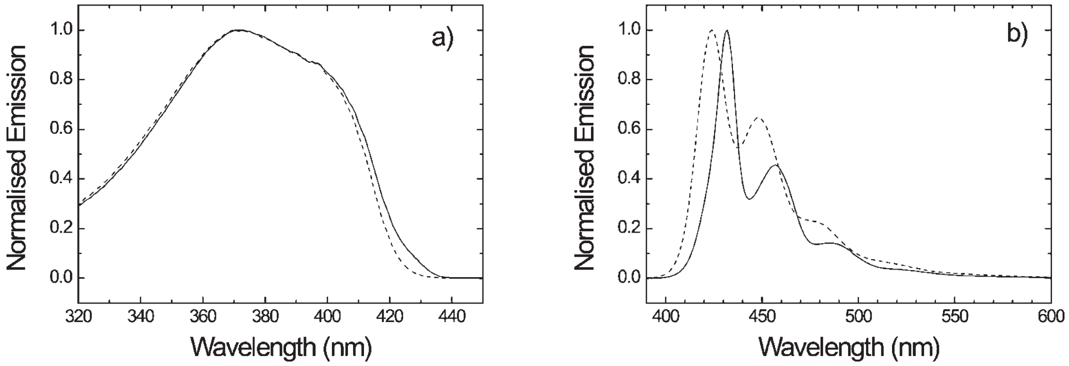

Figure 1. Excitation spectra (a) and emission spectra (b) of a representative PF10 thin film before (dashed line) and after the thermal cycle (solid line).

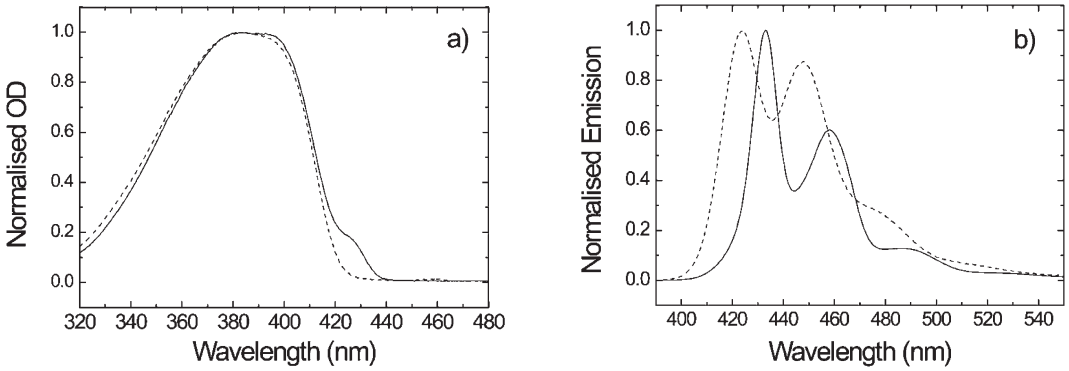

Figure 2. Absorption spectra (a) and emission spectra (b) of a representative PF10 thin film as spun (dotted lines) and after toluene vapor exposure (solid lines).

more the α′ phase identified by Chen et al.[17] more than the classical well-resolved sharp feature observed in PF8 *β* phase.[15,18]

However, the emission spectra clearly show the characteristic well-resolved and red-shifted *β* phase emission.[18] The 0−0 peak shows a red shift from 426 to 433 nm and a narrowing of the primary emission peak from a full width at half-maximum (fwhm) from 21 to 14 nm, which approaches the fwhm for a thermally cycled PF8 film of 10 nm (not shown). All the vibronic replicas exhibit a red shift, indicating a true shift in the energy levels.

Toluene Exposure. After exposure to toluene vapor, the resulting changes in the absorption and emission spectra show very similar changes taking place; a shoulder appears in the absorption spectrum at 429 nm, and the emission spectrum is red-shifted from 426 to 433 nm (Figure 2). The shoulder in the absorption spectrum appears to be of lower intensity than the shoulder in the excitation, which was monitored at 470 nm where contributions are seem from both the α and *β* phase. This is a result of the energy transfer that occurs from the α to the *β* phase for the portion of the spectrum below 420 nm but is not required when the excitation occurs directly on the *β* phase for excitation wavelengths above this. This raises the relative intensity of the *β* phase excitation relative to that of the α phase, an effect which is also seen in PF8.[2] The overall shape of the emission spectrum is almost identical to that produced by thermal cycling.

Low-Temperature Optical Spectra of a Saturated Film. The emission and excitation spectra from a PF10 sample with saturated induced *β* phase by both thermal cycling and toluene vapor exposure were then monitored as a function of temperature. The excitation and absorption spectra of the sample are shown in Figure 3.

The excitation spectra show a main excitation band around 385 nm and shoulders at 410 and 428 nm, the first due to the aggregation of the polymer and the second due to the absorption of the *β* phase.[15] Upon cooling there is red shift of the main absorption band and sharpening of the shoulders due to reduced inhomogeneous broadening. The absorption spectrum shows a clear shoulder at 428 nm, indicating the presence of the *β* phase at an estimated concentration of 0.7% by using the fraction of the absorption band area contribution from the *β* phase peak at 428 nm, found by a multiple-Gaussian fit to the whole absorption band. The emission spectra taken in tandem with the excitation spectra are given in Figure 4.

Emission spectra were collected from excitation at the standard α phase 380 nm absorption band (Figure 4a) and the *β* phase shoulder (Figure 4b). In the case of the *β* phase in PF8 it is well documented that the vibronic band at 455 nm at room temperature becomes resolved into two components. However, there are significant differences in the case of PF10 here. The vibronic bands that form the single peak at 290 K do not become well resolved as is the case for PF8, suggesting a lower degree of ordering as already implied by the greatly reduced content of *β* phase that can be formed in the PF10. If there were some influence of the second vibronic of α phase emission causing this effect, then a small peak would also be seen at 455 nm. Furthermore, in PF8 the emission spectra are similar (not shown) using either excitation at 380 or 432 nm, whereas the PF10 emission shows clear narrowing in the vibronics of the emission spectra when excited directly on the *β* phase absorption band.

Photoluminescence Lifetime. The photoluminescence lifetime was measured for samples with *β* phase induced via the toluene vapor exposure method. A biexponential fit to the peak intensity decay showed a lifetime component in the region 350−400 ps, corresponding to the

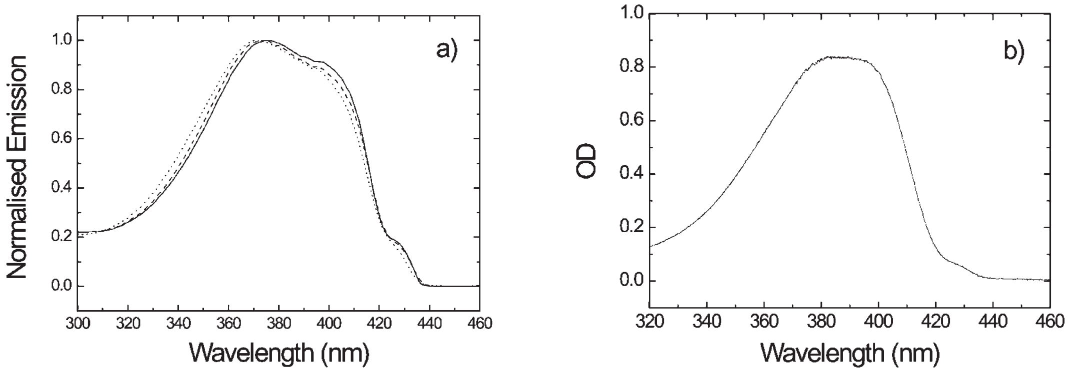

Figure 3. Excitation spectra (a) of the saturated β phase PF10 film at 290 K (dotted line), 150 K (dashed line), and 11 K (solid line) and the sample absorption spectrum (b).

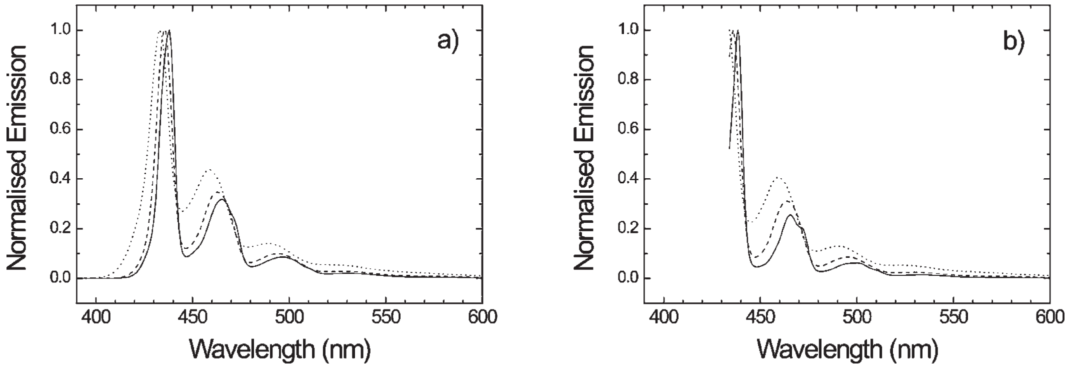

Figure 4. Emission spectra excited at 380 nm (a) of the saturated β phase PF10 film at 290 K (dotted line), 150 K (dashed line), and 11 K (solid line) and the same spectra excited on the β phase absorption at 432 nm (b).

photoluminescence lifetime measured for PF8 in the β phase.[5,10,19] This further supports the observation that the β phase is formed here.

Discussion

Measurements in MCH solution show that in the case of PF10 solution there is no β phase formation. This we ascribe to be due to the high solubility of the alkyl side chains preventing aggregation, as compared to the series PF7−9 where β phase formation in solution can clearly be seen.[15] However, in thin film, where the disruptive effects of the side chain dissolution have been removed, we have been able to form β phase in PF10, albeit at rather lower fraction than in PF7−9.

The two vibronics resolved in the 11 K emission of PF10 were fitted with Gaussian peaks, resulting in fits with energy spacing from the main emission of 164 meV (1323 cm^{-1}) and 203 meV (1641 cm^{-1}) which correspond to the vibrations of carbon−carbon stretching at around 1300 cm^{-1} and symmetric benzene ring stretching around 1600 cm^{-1}. These are the same two vibronics observed in PF8 β phase emission at low temperature. At lower temperatures the symmetric benzene ring stretch becomes more prevalent in relation to the C−C stretch, indicated by a larger relative intensity of the vibronic emission band at 1641 cm^{-1}. This indicates that the C−C stretching mode is reduced at higher temperature. However, this peak never exceeds the height of that at 1323 cm^{-1} as occurs in PF8, indicating that the PF10 does not reach the same high level of ordering.

These results are consistent with the hypothesis we previously proposed[15] that the substituent alkyl chain length strongly governs the formation of the β phase via side chain interactions and that it is the interdigitation of the alkyl side chains the drives the planarization of the polyfluorene backbone. With no disruption from solvent molecules to prevent β phase formation, some β phase formation does occur in PF10 films. This is of interest due to its excellent solubility for solution processing. However, it is still less effective than in the PF8, potentially because it is more difficult to align and interdigitate the longer 10-carbon side chains within the confines of a solid film.

References and Notes

(1) Grell, M.; Bradley, D. D. C.; Long, X.; Chamberlain, T.; Inbasekaran, M.; Woo, E. P.; Soliman, M. *Acta Polym.* **1998**, *49*, 439–444.
(2) Grell, M.; Bradley, D. D. C.; Ungar, G.; Hill, J.; Whitehead, K. S. *Macromolecules* **1999**, *32*, 5810–5817.
(3) Monkman, A. P.; Rothe, C.; King, S. M.; Dias, F. D. In *Polyfluorenes*; Scherf, U., Neher, D., Eds.; Springer: Berlin, 2008; pp 187−226.
(4) Grice, A. W.; Bradley, D. D. C.; Bernius, M. T.; Inbasekaran, M.; Wu, W. W.; Woo, E. P. *Appl. Phys. Lett.* **1998**, *73*, 629–631.
(5) Bradley, D. D. C.; Grell, M.; Long, X.; Mellor, H.; Grice, A.; Inbasekaran, M.; Woo, E. P. In *Optical Probes of Conjugated Polymers*; Vardeny, Z. V., Rothberg, L. J., Eds.; SPIE—Int. Soc. Optical Engineering: Bellingham, 1997; Vol. *3145*, pp 254−259.
(6) Cadby, A. J.; Lane, P. A.; Mellor, H.; Martin, S. J.; Grell, M.; Giebeler, C.; Bradley, D. D. C.; Wohlgenannt, M.; An, C.; Vardeny, Z. V. *Phys. Rev. B* **2000**, *62*, 15604–15609.
(7) Knaapila, M.; Garamus, V. M.; Dias, F. B.; Almasy, L.; Galbrecht, F.; Charas, A.; Morgado, J.; Burrows, H. D.; Scherf, U.; Monkman, A. P. *Macromolecules* **2006**, *39*, 6505–6512.
(8) Knaapila, M.; Torkkeli, M.; Monkman, A. P. *Macromolecules* **2007**, *40*, 3610–3614.
(9) Chunwaschirasiri, W.; Tanto, B.; Huber, D. L.; Winokur, M. J. *Phys. Rev. Lett.* **2005**, *94*, 107402.
(10) Ariu, M.; Sims, M.; Rahn, M. D.; Hill, J.; Fox, A. M.; Lidzey, D. G.; Oda, M.; Cabanillas-Gonzalez, J.; Bradley, D. D. C. *Phys. Rev. B* **2003**, *67*, 195333.
(11) Rothe, C.; King, S. M.; Dias, F.; Monkman, A. P. *Phys. Rev. B* **2004**, *70*, 195213.

(12) Rothe, C.; Galbrecht, F.; Scherf, U.; Monkman, A. *Adv. Mater.* **2006**, *18* (16), 2137.
(13) Winokur, M. J.; Slinker, J.; Huber, D. L. *Phys. Rev. B* **2003**, *67*, 184106.
(14) Knaapila, M.; Dias, F. B.; Garamus, V. M.; Almasy, L.; Torkkeli, M.; Leppanen, K.; Galbrecht, F.; Preis, E.; Burrows, H. D.; Scherf, U.; Monkman, A. P. *Macromolecules* **2007**, *26*, 9398–9405.
(15) Bright, D. W.; Dias, F. B.; Galbrecht, F.; Scherf, U.; Monkman, A. P. *Adv. Funct. Mater.* **2009**, *19* (1), 67–73.
(16) Knaapila, M.; Almasy, L.; Garamus, V. M.; Ramos, M. L.; Justino, L. L. G.; Galbrecht, F.; Preis, E.; Scherf, U.; Burrows, H. D.; Monkman, A. P. *Polymer* **2008**, *49* (8), 2033–2038.
(17) Chen, S. H.; Su, A. C.; Su, C. H.; Chen, S. A. *Macromolecules* **2005**, *38* (2), 379–385.
(18) Dias, F. D.; Morgado, J.; Macanita, A. L.; Costa, F. P.; Burrows, H. D.; Monkman, A. P. *Macromolecules* **2006**, *39*, 5854–5864.
(19) Korovyanko, O. J.; Vardeny, Z. V. *Chem. Phys. Lett.* **2002**, *356* (3−4), 361–367.